THE UNIVERSITY OF MICHIGAN

College of Engineering

Department of Mechanical Engineering

Cavitation and Multiphase Flow Laboratory

Report No. 01357-15-T

BEHAVIOR OF LIQUID SODIUM IN A SINUSOIDAL PRESSURE FIELD

(To be presented at the ASME Symposium on "The Role of Nucleation in Boiling and Cavitation", May, 1970)

by

R. E. Nystrom

F. G. Hammitt

Financial Support Provided by:

National Science Foundation
Grant No. GK-1889

November 1969

ABSTRACT

Utilizing an ultrasonic vibratory cavitation facility, the onset of cavitation was observed in liquid sodium for different liquid sodium temperatures and at various sinusoidal pressure field frequencies. It was observed that the pressure oscillation required to initiate cavitation decreases linearly as the temperature of the sodium is increased from 500 to 1500°F. For frequencies below 20 kHz the cavitation threshold pressure amplitude is essentially independent of frequency. For frequencies above 20 kHz the cavitation threshold begins to increase sharply. Using the onset of cavitation data and the saturation temperature-pressure data for liquid sodium, the superheat required to produce nucleate boiling in liquid sodium was calculated. As the saturation temperature of liquid sodium is increased the calculated superheat decreases. For frequencies below 20 kHz the calculated sodium superheat requirements, which are independent of frequency, are in good agreement with steady-state sodium superheat data reported in the literature.

TABLE OF CONTENTS

LIST OF FIGURES

LIST OF TABLES

NOMENCLATURE

A	Maximum tip amplitude
a	Vessel radius
b	Test specimen radius
C	Sound velocity in liquid
f	Frequency of applied field
$\bar{H}_j$	$\bar{K}_j \sin \bar{K}_j$
J_o, J_1	Bessel functions of the first kind of order zero and one
$\bar{k}$	$a\bar{\omega}$
$\bar{K}_j$	$\bar{\ell}\,(\bar{k}^2 - \bar{\alpha}_j^2)^{1/2}$
ℓ	Length of closed vessel
P	Pressure at a point $(\bar{r}, \bar{z})$ in the liquid at time
P_a	Argon cover gas pressure
P_g	Partial pressure of undissolved gas within bubble
P_L	Liquid pressure
P_o	Sinusoidal pressure pulse amplitude
P_s	Saturation vapor pressure
P_v	Vapor pressure
P_a	Atmospheric Pressure
R	Bubble radius
R'	Effective bubble radius
r	Radius coordinate of point in liquid
T	Period of pressure wave
T_v	Liquid temperature
T_{sat}	Saturation temperature corresponding to P_L
t	Time
U_o	Maximum velocity of test specimen

z	Axial coordinate of point in liquid
z_o	$P_o + P_s - P_a$
α_j	j-th zero of J_1
η	Viscosity
λ	b/a
ρ, ρ_o	Liquid density
σ	Liquid surface tension
τ	T/2
ω	Angular frequency of vibration

Sub- and Superscripts

$(\bar{\ })$	Dimensionless quantity
$(\dot{\ })$	Derivative with respect to time
$(\ )_j$	Index

I. INTRODUCTION

With the development of sodium cooled fast breeder nuclear reactors, renewed emphasis has been placed on determining the heat transfer characteristics of liquid sodium. The determination of the boiling properties of a reactor coolant is necessary since changes in the coolant "void fraction" affect the nuclear reactivity, thus affecting the reactor power output. Generation of a coolant void fraction generally occurs when the fuel element temperature is increased sufficiently to produce nucleate boiling within the bulk of the coolant. Thus if the reactor temperature is increased so that nucleate boiling occurs, the void fraction increases producing a change in the nuclear reactivity. If the reactor has a "positive void coefficient", an increase in the void fraction produces an increase in reactivity which in turn produces a further increase in temperature, thus leading to a serious instability. This situation is especially critical in fast breeder reactors since large changes in reactivity may lead to an extremely rapid increase in the reactor power output.

Nucleate boiling is characterized by two separate processes: the formation of bubbles (nucleation), and the subsequent growth of these bubbles. For the first process to occur there must exist, in the liquid, sites or locations from which the bubbles can nucleate. Consistent with most current literature, we have assumed that these sites are small spherical vapor bubbles somehow stabilized in the liquid. A force balance on a spherical vapor bubble of radius R in unstable equilibrium in a liquid indicates that

$$P_v - P_L = 2\sigma/R \tag{1}$$

where P_v = vapor pressure inside bubble

P_L = liquid pressure

σ = surface tension

R = bubble radius.

Unstable equilibrium exists in that for a bubble of radius less than R, eq. (1) is no longer satisfied and the bubble will collapse. For a bubble of radius larger than R, eq. (1) is again no longer satisfied and the bubble will grow. Thus, if the conditions in the liquid are such that eq. (1) is satisfied and then there is a slight increase in R, bubble growth will occur.

In the idealized heat transfer case nucleate boiling in a liquid is produced under constant liquid pressure, P_L, by increasing the liquid temperature, T_v, until the saturation pressure corresponding to the liquid temperature (which for thermal equilibrium in the liquid is identical to P_v) satisfies eq. (1). At this point the liquid is in a superheated condition since the liquid temperature is above the saturation temperature corresponding to the liquid pressure. The required superheat becomes the difference between the liquid temperature, T_v, and the saturation temperature corresponding to P_L

Eq. (1) can also be satisfied by maintaining the liquid temperature constant, thereby keeping P_v constant, and then lowering the surrounding liquid pressure, P_L, until eq. (1) is satisfied and bubble growth occurs. This would be the idealized cavitation case. Superheat can be defined in the same manner as for the heat transfer case except that T_v is assumed constant, and the lower temperature of concern becomes the saturation temperature corresponding to the reduced liquid pressure, P_L. Using this cavitation technique to study superheat requirements for nucleate boiling provides the advantage of allowing the application of the required changes in liquid pressure in a very short time. For example, if an ultrasonic transducer is used to transmit a 20 kHz

pressure wave through the liquid, the duration of the negative pressure pulse producing the cavitation or nucleate boiling in the liquid is only 25 microseconds. Ultrasonic cavitation techniques were used in the present experiment to determine the time dependence of the superheat requirements for nucleate boiling in liquid sodium on the liquid saturation temperature and on the frequency of the applied sinusoidal pressure field.

II. EXPERIMENTAL EQUIPMENT

The University of Michigan high-temperature ultrasonic vibratory facility, initially developed by Garcia,[1, 2] was modified for this experiment.[3] A brief description of the modified facility is included for convenience.

Fig. 1 is a schematic diagram of the modified facility. The sinusoidal voltage signal, supplied by a variable frequency audio-oscillator, is amplified and applied to a lead-zirconate-titanate electrostrictive piezoelectric crystal, the displacements of which are amplified by the "exponential horn" portion of the assembly. The axial motion of the tip of the "test specimen"* produces pressure waves in the test fluid. If the negative portion of these waves is such that the local liquid pressure is reduced sufficiently, "cavitation" or "boiling" will occur in the test fluid. A cover gas system is employed to provide the required atmosphere and pressure above the test fluid in the cavitation vessel. Fig. 2 is a photograph of the facility.

---

*Nomenclature applies to the conventional use of this apparatus for cavitation damage tests.

III. PRESSURE FIELD ANALYSIS

The cavitation vessel which contains the test fluid is a stainless steel right circular cylinder. A circular baffle plate is mounted to the vessel top plate so that the bottom surface of the test specimen is flush with the bottom surface of the baffle plate (Fig. 3). This baffle-plate geometry was used to allow a mathematical analysis of the pressure field as explained below.

If A is the maximum tip amplitude, the tip displacement at any time is then $A \sin(\omega t)$, and its velocity is $U_o \cos(\omega t)$, where ω is the angular frequency of vibration and $U_o = \omega A$ is the maximum velocity of the test specimen.

The analysis developed by Lansing et al [4] was used to determine the amplitude of the pressure field at any point within the vessel. Neglecting viscosity and other dissipative mechanisms, and assuming rigid vessel walls, the acoustic wave equation was solved and the following expression obtained:

$$P(\bar{r}, \bar{z}, t) = \bar{\ell}\,\bar{k}\,\rho_o U_o C \left\{ \frac{\lambda^2 \cos\left[\bar{\ell}\,\bar{k}\,(1-\bar{z})\right]}{\bar{\ell}\,\bar{k}\,\sin\left[\bar{\ell}\,\bar{k}\right]} + 2\lambda \sum_{j=1}^{\infty} \frac{\cos\left[\bar{K}_j (1-\bar{z})\right] J_o(\alpha_j \bar{r})\, J_1(\alpha_j \lambda)}{\alpha_j \bar{H}_j J_o^2(\alpha_j)} \right\} \sin \omega t \qquad (2)$$

where

$\bar{r} = r/a$

$\bar{\ell} = \ell/a$

$\bar{z} = z/\ell$

$\bar{k} = a\bar{\omega}$

$\bar{\omega} = \omega/C$

$\lambda = b/a$

$\bar{K}_j = \bar{\ell}\,(\bar{k}^2 - \alpha_j^2)^{1/2}$

α_j = j-th zero of J_1

J_1 = Bessel function of the first kind of order one.

J_o = Bessel function of the first kind of order zero

$\bar{H}_j = \bar{K}_j \sin \bar{K}_j$.

Eq. (2) indicates that longitudinal resonant conditions exist when $\sin(\bar{\ell}\bar{k}) = 0$, transverse modes occur whenever $\bar{K}_j = 0$, and longitudinal and transverse modes occur when $\sin \bar{K}_j = 0$. Eq. (2) may be used to determine the pressure field inside the vessel only if conditions are far removed from any resonant condition, since eq. (2) predicts infinite pressure at resonance.

Eq. (2) contains the geometrical parameters, fluid density, and velocity of sound, which are known functions of temperature, frequency of applied voltage, and horn amplitude. This last quantity was measured using the output voltage from the lead-zirconate-titanate piezoelectric crystal mounted on the top of the assembly. This output voltage is proportional to the test specimen displacement. Calibration was obtained using a KD-38 Fotonic Sensor* to monitor the horn tip displacement in air.[2]

To verify eq. (2), the pressure field was measured in water using a microprobe described elsewhere,[2] especially developed for this task. Fig. 4 compares a typical set of experimental pressure points with the theoretical curve from eq. (2). Because of the close agreement obtained, and since the fluid properties of water and sodium are quite similar, eq. (2) was used to determine the pressure field in the cavitation vessel with either water or liquid sodium as the test fluid.

---

* MTI Instruments Division, Latham, New York.

IV. EXPERIMENTAL INVESTIGATIONS IN LIQUID SODIUM

For the sodium tests, horn assemblies of differing resonant frequencies (14, 20, 22, and 25 kHz) were used to investigate the frequency dependence of the cavitation threshold pressure oscillation. For each transducer horn assembly the effective length of the cavitation vessel was adjusted such that conditions inside the vessel would be far removed from resonance.

The horn tip units ("test specimens") were of 304 stainless steel, with bottom surfaces machined in a lathe to an approximate 32 μ-inch finish, comparable in roughness to drawn tubing.[4] An acoustic probe especially developed for this purpose, connected to a vacuum tube voltmeter and a dual beam oscilloscope, was used to detect the onset of cavitation. This technique is common in many places.[5] The argon cover gas was maintained at a pressure of 15.0 psia, providing a slight overpressure to prevent air leakage into the cavitation vessel. New sealed sodium ingots were loaded into the vessel in a dry box under argon for each test series, using the technique previously developed in this laboratory for lithium.[1, 2]

The temperature of the liquid sodium was raised to 500°F after the vessel was placed in the furnace. With the sodium temperature held constant at 500°F, the input power to the transducer horn assembly was slowly and continuously increased until the onset of cavitation was determined by the acoustic probe. The power to the transducer horn assembly was then decreased to zero. The counterweight crystal (Fig. 1) output voltage at the onset of cavitation was observed (using a vacuum tube voltmeter) to determine horn tip amplitude. This process was repeated ten times while maintaining the temperature constant at 500°F. The resulting ten values of counterweight crystal voltage at the onset of cavitation were averaged to obtain one data point for the onset of cavitation at 500°F. The temperature was then increased to 750°F and the onset of cavitation was again determined

a total of ten times, and these values averaged to obtain a data point for the onset of cavitation at 750°F. This process was repeated at approximately 1000, 1250, and 1500°F. To determine repeatability, the entire procedure was again repeated using the same charge of sodium and the same transducer horn assembly.

The entire process as described above was performed for each of the four exponential horns using a new 304 stainless steel test specimen and a fresh charge of sodium for each horn. Finally, an additional check run was made for each of the four exponential horns to further check repeatability. A fresh charge of sodium and a new test specimen were used for each of the four check runs.

Upon completion of the last data run using liquid sodium as the test fluid, the cavitation vessel was removed from the furnace and delivered to Atomic Power Development Associates, Inc., Detroit, Michigan, for analysis of the sodium. Table 1 lists the oxygen, hydrogen, and carbon content of the sodium used in the last data run. This can be considered a typical run, since the procedures followed for all runs were identical. Table 1 also lists impurities found in sodium samples taken from the Enrico Fermi sodium cooled fast reactor, indicating that the sodium in our tests at their conclusion was approximately of reactor grade.

Figs. 5, 6, 7, and 8 show the onset of cavitation data using the 14, 20, 22, and 25 kHz transducer horn assemblies, respectively. The peak pressures of the applied sinusoidal pressure wave are obtained from eq. (2) when evaluated at the point $r = 0$ and $z = 0$. The test specimen displacement was obtained from the counterweight crystal calibration curves using the counterweight crystal voltages observed at the onset of cavitation. A least mean square analysis was used to establish the linear relationship between applied changes in pressure and liquid temperature at the onset of cavitation. Similar

linear relationships have been reported in the literature where water was used as the test fluid.[6, 7] To determine the frequency dependence the data from Figs. 5, 6, 7, and 8 were replotted in Fig. 9 as peak values of sinusoidal pressure vs. frequency for various liquid sodium temperatures.

V. DISCUSSION OF RESULTS

In reviewing the experimental data the frequency and temperature dependence are of major interest.

A. Frequency Dependence

As the frequency of the applied pressure field is increased, the observed cavitation thresholds increase (Fig. 9) at an increasing rate for frequencies above approximately 20 kHz, i.e., there is relatively little frequency dependence on the cavitation thresholds for frequencies below 20 kHz. For frequencies above 20 kHz the cavitation thresholds begin to increase sharply.

Boguslavskii and Korets[8] provide the most comprehensive theoretical investigation of the effect of frequency on the cavitation threshold. They considered the influence of the inertial and viscous forces on the motion of vapor cavities in an incompressible liquid under the action of an alternating pressure field. In order to discuss the frequency dependence a partial review of their analysis will be given here.

Starting with the Noltingk-Neppiras equation[9, 10] describing the growth of a vapor cavity, we have

$$\rho\left(R\ddot{R} + \frac{3}{2}\dot{R}^2\right) + \frac{2\sigma}{R} + 4\eta\frac{\dot{R}}{R} = P_o \sin\omega t + P_s - P_a \qquad (3)$$

where ρ = density of fluid

R = radius of vapor bubble

σ = surface tension

η = dynamic viscosity

$P_o \sin \omega t$ = applied pressure field

P_s = saturation vapor pressure

P_a = atmospheric pressure

ω = $2\pi f$

f = frequency of applied field.

Boguslavskii and Korets approximated the sinusoidal pressure field by a square wave variation, with the dilation and compression pulses possessing an amplitude P_o for a time $\tau = T/2$ where $T=2\pi/\omega$. If eq. (3) is written for the dilation pulse we have with the square wave approximation

$$\rho(R\ddot{R} + \frac{3}{2}\dot{R}^2) + \frac{2\sigma}{R} + 4\eta\frac{\dot{R}}{R} = \mathcal{Z}_o \qquad (4)$$

where $\mathcal{Z}_o = P_o + P_s - P_a$

is the tension applied to the liquid during the dilation pulse. The first term of eq. (4) is the inertial term and has an order of magnitude $\rho\bar{R}^2/\tau^2$ where $\bar{R}$ represents the radius of the bubble at the end of the dilation period τ. The second term is the surface tension term, and the third represents the effects of viscosity, having an order of magnitude $4\eta/\tau$. Boguslavskii defines the onset of cavitation as the point at which the incipient nuclei with radius of approximately 10^{-4} cm grow to a radius of the order $\bar{R} = 5 \times 10^{-2}$ cm during the time τ. This choice of $\bar{R}$ is consistent with the work of Noltingk and Neppiras.[9,10]

Using liquid sodium as the test fluid it is found that the surface tension term is approximately 3 atmospheres, using σ = 148 dynes/cm, an average value for the temperature range of 500 to 1500°F. The inertial term reaches 3 atmospheres when the frequency is increased to approximately 17.5 kHz. The viscous term

($\eta = 0.41 \times 10^{-2}$ poise) does not reach 3 atmospheres until the frequency reaches approximately 10^8 Hz, and therefore remains relatively negligible for the present investigation. Using the above analysis and assuming an initial radius of 10^{-4} cm, it appears that the cavitation threshold for liquid sodium is essentially independent of frequency until the frequency reaches approximately 15-20 kHz. The cavitation threshold then becomes significantly frequency-dependent, and increases substantially for increases in frequency above 15-20 kHz. These theoretical predictions are obviously quite consistent with our measured data (Fig. 9). It should be pointed out that the choice of the initial bubble size for liquid sodium is somewhat arbitrary. However, as mentioned later, if one assumes that spherical vapor bubbles serve as nucleation sites, the radii of these bubbles from these experiments is shown to be on the order of 10^{-4} cm, as was assumed in the preceding analysis.

B. Temperature Dependence

The required liquid pressure oscillation to provide cavitation initiation was observed to decrease approximately linearly with temperature. This temperature dependence can be understood by considering the effects of a change in temperature on the physical properties of the fluid, namely vapor pressure, surface tension, viscosity, and gas content.

If it is assumed that the spherical bubbles serving as nucleation sites contain a small amount of undissolved gas, then eq. (1) becomes

$$P_v + P_g - P_L = 2\sigma/R \tag{5}$$

where P_g is the partial pressure of the undissolved gas within the bubble. Thus an increase in the partial pressure P_g reduces the required

change in P_L necessary to produce cavitation. Galloway[7] observed cavitation thresholds for water and benzene while varying the per cent air concentrations. He reported a linear increase in the cavitation threshold as the air concentration was decreased from 100 per cent to approximately 5 per cent. The solubility of argon in liquid sodium[11] at 1 atm and 480°C is about 0.4×10^{-8} atom fraction and increases by an extrapolated factor of about 10^2 to 1500°F, giving a volume percent at 1500°F and 1 atm of about 0.001% vs. about 1-2% for air in water at room temperature. Nevertheless, this large increase in solubility with temperature for sodium may tend to reduce the cavitation threshold requirements even though the solubilities are very small at all temperatures.

The vapor pressure P_v for the test fluid of course increases as the temperature of the test fluid is increased. From eq. (5) it can be seen that if P_v is increased the required change in the local liquid pressure necessary to produce bubble growth is reduced, since the argon over-pressure was maintained constant for all tests. For liquid sodium $P_v = 5.15 \times 10^{-4}$ psi at 500°F and $P_v = 1.86$ psi at 1500°F.[12] Therefore, this relative change in P_v, large compared to the absolute pressure, contributes to the observed temperature dependence.

The surface tension for liquid sodium decreases linearly from 176 dynes/cm at 500°F to 120 dynes/cm at 1500°F.[12] From eq. (5) it can be seen that this decrease in surface tension results in reducing the change in pressure requirements necessary to produce cavitation.

It was pointed out earlier that the viscosity effect on bubble behavior was small compared to inertial and surface tension effects for frequencies of interest. Briggs et al[13] compared the cavitation threshold strengths of liquids with varying values of viscosity and

found that the cavitation threshold decreased slightly with a decrease in viscosity. The viscosity of liquid sodium decreases from 0.41×10^{-2} poise at $500^{o}F$ to 0.17×10^{-2} poise at $1500^{o}F$.[12] The reduction in viscosity may also contribute to the decrease in cavitation threshold for an increase in temperature; however, this effect is probably small.

VI. CONVERSION TO SUPERHEAT REQUIREMENTS

Fig. 10 illustrates the relationships among the vapor pressure P_v, the argon cover gas pressure P_a, and the applied pressure field $P_o \sin \omega t$. The applied sinusoidal pressure field alternates about the applied cover gas pressure which for the present experiment was maintained at 15.0 psia. With the application of the alternating pressure field, the liquid pressure P_L becomes

$$P_L = P_a - P_o \sin \omega t. \tag{6}$$

As shown in Fig. 10 the liquid pressure must be reduced to some value below the vapor pressure to satisfy eq. (1) and to initiate cavitation in the liquid. If it is assumed that the liquid responds approximately to the peak value of the sinusoidal pressure field, then substituting eq. (6) into eq. (1) we obtain at the onset of cavitation

$$P_o + P_v - P_a = 2\sigma/R \tag{7}$$

P_o is determined from the data recorded at the onset of cavitation. P_v and σ, which are functions of temperature, are known quantities. P_a was held constant at 15.0 psia. Thus the radius of the vapor bubble which serves as the nucleation site

becomes the only unknown quantity, and can be determined from eq. (7). In other words, for the range below about 20 kHz where frequency effects are small, by determining the liquid pressure oscillation required to produce cavitation, the radius of the vapor bubble existing in the liquid which serves as a nucleation site can be determined. For frequencies above about 20 kHz, as previously stated, inertial effects become important and begin to affect the cavitation threshold, so that pressure oscillation for cavitation initiation is affected not only by R_o, but also by inertial effects. Thus at higher frequencies, an effective bubble radius R' must be utilized, if the equation

$$P_o + P_v - P_a = 2\sigma/R' \tag{7a}$$

is to be used for all frequencies. For frequencies below 20 kHz the effective radius R' is equal to the radius of the bubble serving as the nucleation site, if this is indeed a spherical bubble. For frequencies above 20 kHz, R' represents an effective radius which takes into account inertial and possible viscous effects. Thus R' is smaller than the actual radius R_o for high frequencies.

We have then the following steps in converting the onset of cavitation data to superheat requirements:

1. From the onset of cavitation data determine the corresponding quantity $2\sigma/R'$ using eq. (7a).

2. Identify the temperature of the liquid at the onset of cavitation as the temperature T_v.

3. For a particular value of T_v determine the difference between the saturation pressure corresponding to T_v and the value of $2\sigma/R'$ determined from the cavitation data for the chosen value of T_v. This difference becomes the saturation pressure corresponding to T_{sat}.

4. From the curve of saturation pressure versus saturation temperature for liquid sodium determine T_{sat}. The temperature difference $T_v - T_{sat}$ is then the required superheat. The interpretation of this superheat requirement is that liquid sodium with a boiling point of T_{sat} must be heated to T_v before nucleate boiling occurs in the liquid. This change in temperature would be applied as a sinusoidal temperature change with a frequency equal to the frequency of the pressure field used to obtain the cavitation data used in step 3 above.

Following these steps, the onset of cavitation data shown in Fig. 9 were converted to sodium superheat requirements. Shown in Fig. 11 are curves of $2\sigma/R'$ versus T_v for 14.0, 17.5, 21.0, and 24.5 kHz. The curves of $2\sigma/R'$ were determined using the data in Fig. 9 and eq. (7a). Listed in Table 2 are the numerical values used in the calculation of the sodium superheat. It was necessary to extrapolate the $2\sigma/R'$ curves for the 21.0 and 24.5 kHz frequencies since at relatively low temperatures the resulting difference between the saturation pressure corresponding to T_v and the quantity $2\sigma/R'$ becomes negative and cannot be used as a saturation pressure for T_{sat}. Plotted in Fig. 12 are the resulting curves of superheat versus liquid sodium saturation temperature for 14.0, 17.5, 21.0, and 24.5 kHz. To indicate the frequency dependence the data in Fig. 12 were replotted in Fig. 13 as curves of superheat requirements versus frequency for the saturation temperatures of 500, 750, 1000, 1250, and 1500°F.

VII. DISCUSSION OF SUPERHEAT RESULTS

From the curves of $2\sigma/R'$ versus sodium temperature, the effective bubble radius R' can be determined. Knowing the values of surface tension as a function of temperature, the effective

radius R' was calculated and varies from 0.80×10^{-4} cm at 500°F and 24.5 kHz to 31.7×10^{-4} cm at 1500°F and 14 kHz (Table 2). For constant frequency the effective bubble radius R' increases for increasing temperature. For example, at 14 kHz the effective bubble radius increases from 1.93×10^{-4} cm at 500°F to 31.7×10^{-4} cm at 1500°F. In other words, as the temperature at which boiling occurs in the liquid is increased, the effective radius of the bubble serving as the nucleation site appears to increase. Physically, this is reasonable for several reasons. As the temperature is increased, the surface tension is reduced, tending to increase the radius of the bubble stabilized in the liquid. The vapor pressure P_v increases with temperature with the possible result that the radius of the bubble would be increased. The solubility of argon in liquid sodium increases with temperature and this solubility may contribute to a larger radius for the bubble stabilized in the fluid. However, it should be emphasized that the mechanisms involved in the stabilization of these spherical bubbles are not known and the exact effect of the changes in the above mentioned variables cannot be determined, although the trends outlined above appear reasonable in accounting for the increase in R' for an increase in temperature.

It is noted that for a constant liquid sodium temperature the effective radius R' decreases for increasing frequency. As discussed in the previous section this decrease in R' is due to the frequency dependence of the required onset pressures, and is presumably primarily a result of inertial resistance to bubble growth in the liquid.

In reviewing the numerical values calculated for the effective bubble radius it is observed that for temperatures below 1000°F, the values of R' are on the order of 10^{-4} cm, which was the value assumed

for the radius in the previous discussion on frequency dependence, lending credence to the present experimentally determined values of R'.

Fig. 12 indicates that as the saturation temperature is increased the required superheat decreases. This is primarily due to two effects. First, the superheat requirement increases with the quantity $2\sigma/R'$, and $2\sigma/R'$ decreases for increasing sodium temperature (Fig. 11). Second, from the saturation curve for liquid sodium, for a constant change in pressure the corresponding changes in saturation temperature decrease for higher liquid temperatures.[12] In other words, because of the nonlinearity of the saturation curve for sodium (typical of most liquids), a given change in pressure required to produced cavitation results in a much larger superheat requirement for a relatively low value of temperature than for a high value of temperature. Therefore, the combination of the reduction in the measured $2\sigma/R'$ for increasing liquid sodium temperature and the nonlinearity of the saturation line for liquid sodium results in a decrease in superheat for an increase in saturation temperature.

The superheat requirements for frequencies from 14 to approximately 18 kHz are essentially independent of frequency (Fig. 13) and as such should be comparable to superheat requirements determined from steady state heat transfer experiments. The majority of the sodium superheat measurements reported in the literature were made in essentially steady state heat transfer experiments in which the increase in temperature necessary to produce boiling in the liquid sodium was applied over relatively long periods of time compared to the application times utilized in this study. Holtz and Singer[14] presented a comparison of currently available data on sodium superheating taken from seven different sources. The majority of the superheats reported by Holtz and Singer lie within the shaded area

shown in Fig. 12. In comparing the results of this investigation with the data represented by the shaded area in Fig. 12 it is noted that the curves of superheat requirements for the frequencies 14 and 17.5 kHz are within this shaded area for saturation temperatures from approximately 1150 to 1600°F. In other words, there appears to be reasonably good agreement between the lower frequency portion of the data of this study and the relatively steady state data reported in the literature for comparable value of T_{sat}. It would be difficult to obtain a more exact comparison because of the many variables that can affect supherheat behavior of liquid sodium. As discussed by Fauske[15] these variables include heat flux, heating surface, fluid velocity, pressure, pressure-temperature history, aging, purity, radiation, and heating method. However, it is encouraging to note that the sodium superheat data obtained using cavitation techniques does fall within the range of superheat data obtained using heat transfer techniques.

VIII. CONCLUSIONS

(1) A method has been developed to determine the change in liquid pressure at relatively high frequency required to initiate cavitation in liquid sodium. This change in liquid pressure was determined as a function of the liquid sodium temperature and as a function of the frequency of the applied sinusoidal pressure field. It was observed that the cavitation threshold decreases approximately linearly as the liquid sodium temperature is increased from 500 to 1500°F. For frequencies below approximately 20 kHz the cavitation threshold was found to be essentially independent of frequency. For frequencies above 20 kHz the cavitation threshold begins to increase sharply.

(2) Utilizing the effective radii of the spherical bubbles which are assumed to serve as nucleation sites for the onset of

cavitation, the superheat requirements for liquid sodium were determined. It was calculated that, as the saturation temperature of the liquid sodium is increased, the resulting superheat requirements decrease. The calculated values of sodium superheat for frequencies below 20 kHz which are independent of frequency are in good agreement with steady-state sodium superheat data found in the literature.

(3) The results obtained in this study can be related to conditions which may arise in a sodium cooled nuclear reactor. The purity of the sodium used in this study was comparable to the purity of liquid sodium used in fast breeder nuclear reactors. The bottom surfaces of the test specimens used in this study were machined in a lathe to a commerically smooth condition so that their roughness is approximately comparable to that of the sodium containment surfaces found in nuclear reactors.

ACKNOWLEDGEMENTS

The authors would like to acknowledge the financial support of the National Science Foundation (Grant No.GK-1889) which provided support for this work. The authors wish to thank Dr. Robert Cheesewright (on leave in the Nuclear Engineering Department, the University of Michigan, during this period) of Queen Mary College, University of London, London, England, for his many helpful suggestions.

The authors are also grateful to Mr. Alton E. Klickman of the Atomic Power Development Associates, Inc. of Detroit, Michigan, for the sodium analysis and for his interest in the study. Thanks are due also to Mr. Edward Rupke, Instrument Shop Supervisor, and Mr. William Rekewitz, Instrument Shop Foreman, for many helpful suggestions and fabrication of the necessary hardware.

REFERENCES

1. Garcia, R., "Comprehensive Cavitation Damage Data for Water and Various Liquid Metals Including Correlations with Material and Fluid Properties," Ph. D. Thesis and ORA Technical Report No. 05031-6-T, Department of Nuclear Engineering, University of Michigan, August, 1966.

2. Garcia, R., Hammitt, F. G., "Cavitation Damage and Correlations with Materials and Fluid Properties", Trans. ASME, J. Basic Engr., D, 89, 4, 753-763, 1967.

3. Nystrom, R. E., "Ultrasonically Induced Sodium Superheat," Ph. D. Thesis and ORA Technical Report 01357-8-T, Department of Nuclear Engineering, The University of Michigan, May, 1969.

4. Lansing, D. L., Watkins, C. E., and Kantarges, G. T., "Oscillating Pressures within a Cylindrical Chamber That Has a Circular Piston in one End Wall", Journal of the Acoustical Society of America, Vol. 36, No. 11, November, 1964, pp. 2222-2232.

5. Mechanical Design and Systems Handbook, H. A. Rothbart, Editor-in-Chief, McGraw-Hill Book Co., New York, 1964, pp. 19-23.

6. Blake, F. G., Jr., "The Onset of Cavitation in Liquids," Technical Memo No. 12, Acoustics Research Laboratory, Harvard University, Cambridge, Mass., 1949.

7. Galloway, W. J., "An Experimental Study of Acoustically Induced Cavitation in Liquids," Journal of the Acoustical Society of America, Vol. 26, No. 5, September, 1954, pp. 849-857.

8. Boguslavskii, Yu., and Korets, V. L., "Cavitation Threshold and its Frequency Dependence," Soviet Physics-Acoustics, Vol. 12, No. 4, April-June, 1967, pp. 364-368.

9. Noltingk, B. E., and Neppiras, E. A., "Cavitation Produced by Ultrasonics," Proc. Phy. Soc. (London), Vol. B63, 1950, pp. 674-685.

10. Neppiras, E. A., and Noltingk, B. E., "Cavitation Produced by Ultrasonics: Theoretical Condition for the Onset of Cavitation," Proc. Phy. Soc. (London), Vol. B64, 1951, pp. 1032-1038.

11. Vogal, R. C., Levenson, M., Proud, E. R., Royal, J., Argonne National Laboratory, Chem. Engr. Div. Semi-Annual Progress Report, July-Dec. 1966, pp. 128-131, ANL-7325, Argonne National Laboratory, Argonne, Illinois, April, 1967.

12. Dunning, E. L., "The Thermodynamic and Transport Properties of Sodium and Sodium Vapor", ANL-6246, Argonne National Laboratory, October, 1960.

13. Briggs, H. B., Johnson, J. B., and Mason, W. P., "Properties of Liquids at High Sound Pressures," Journal of the Acoustical Society of America, Vol. 19, No. 4, 1947, pp. 664-677.

14. Holtz, R. E., and Singer, R. M., "On the Superheating of Sodium at Low Heat Fluxes," ANL-7383, Argonne National Laboratory, Argonne, Illinois, November, 1967.

15. Fauske, H. K., "Liquid Metal Boiling in Relation to LMFBR Safety Design," Presented at the Tenth National Heat Transfer Conference A. I. Ch. E.-ASME, Philadelphia, Pennsylvania, August 11-14, 1968.

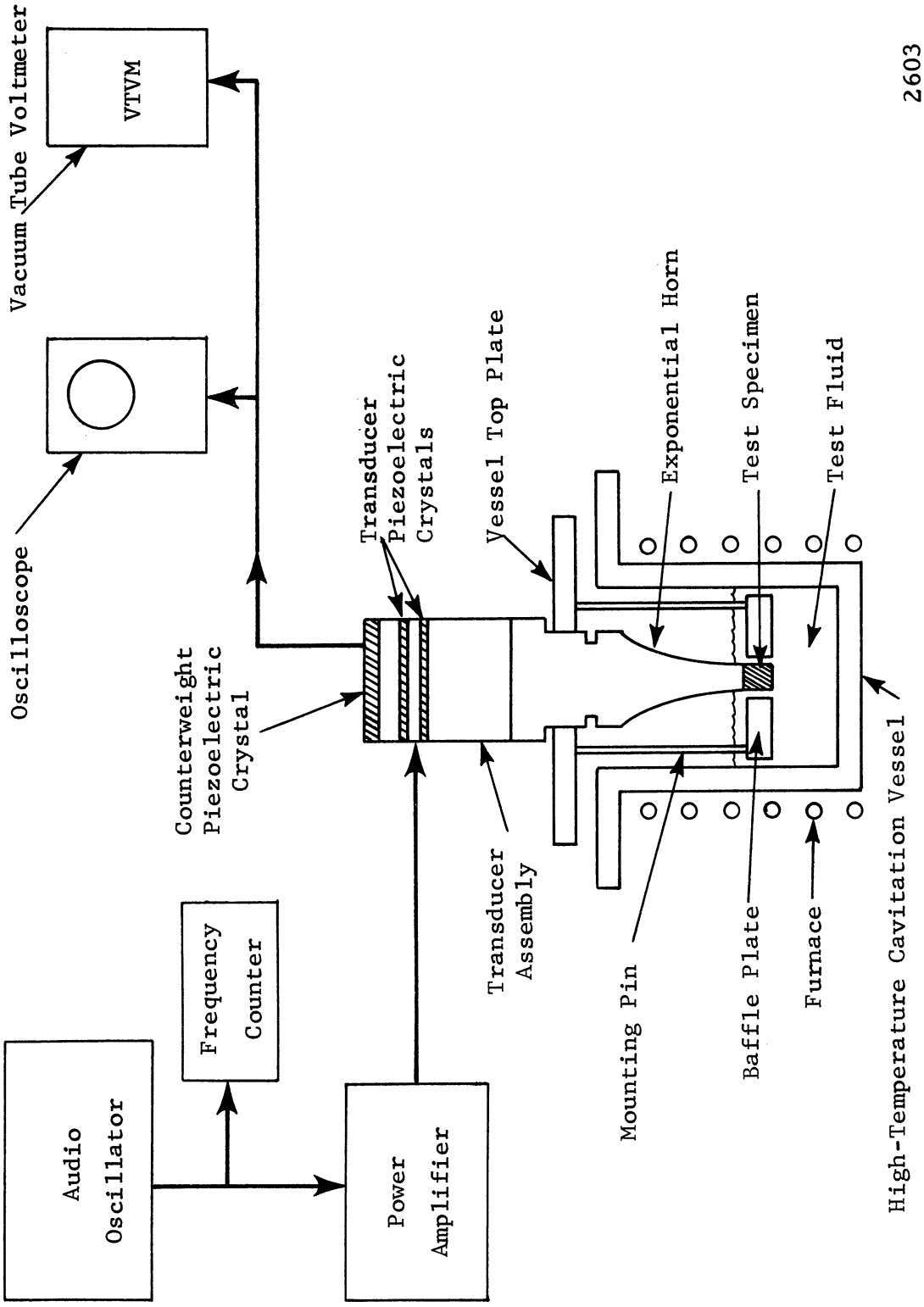

Figure 1. Block Diagram of the High-Temperature Ultrasonic Vibratory Facility

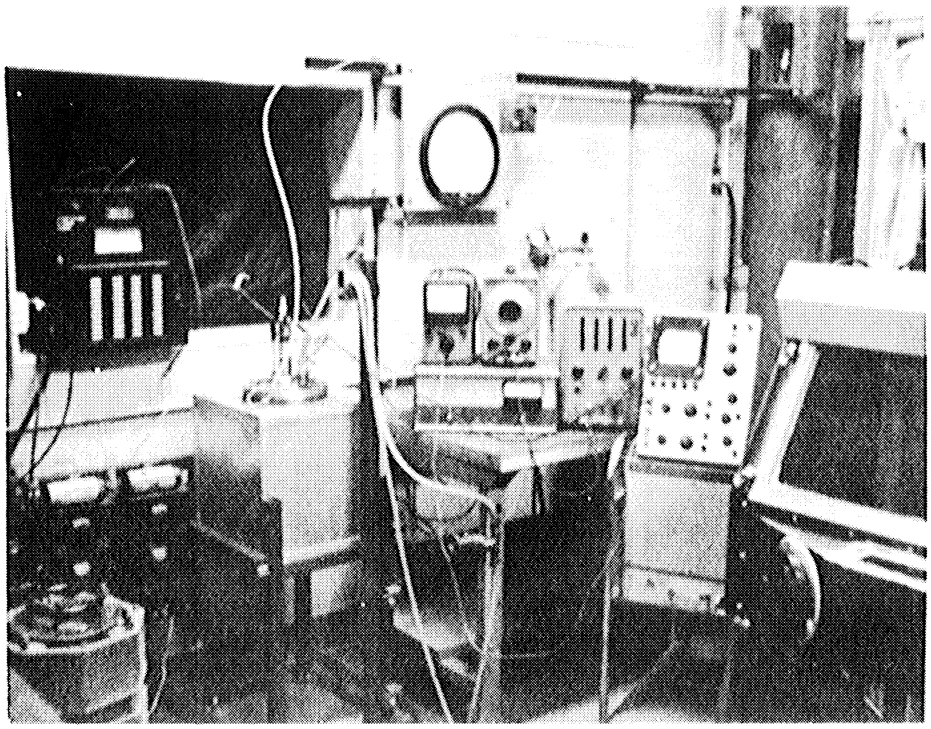

2604

Figure 2. Photograph of the High-Temperature Ultrasonic Cavitation Facility

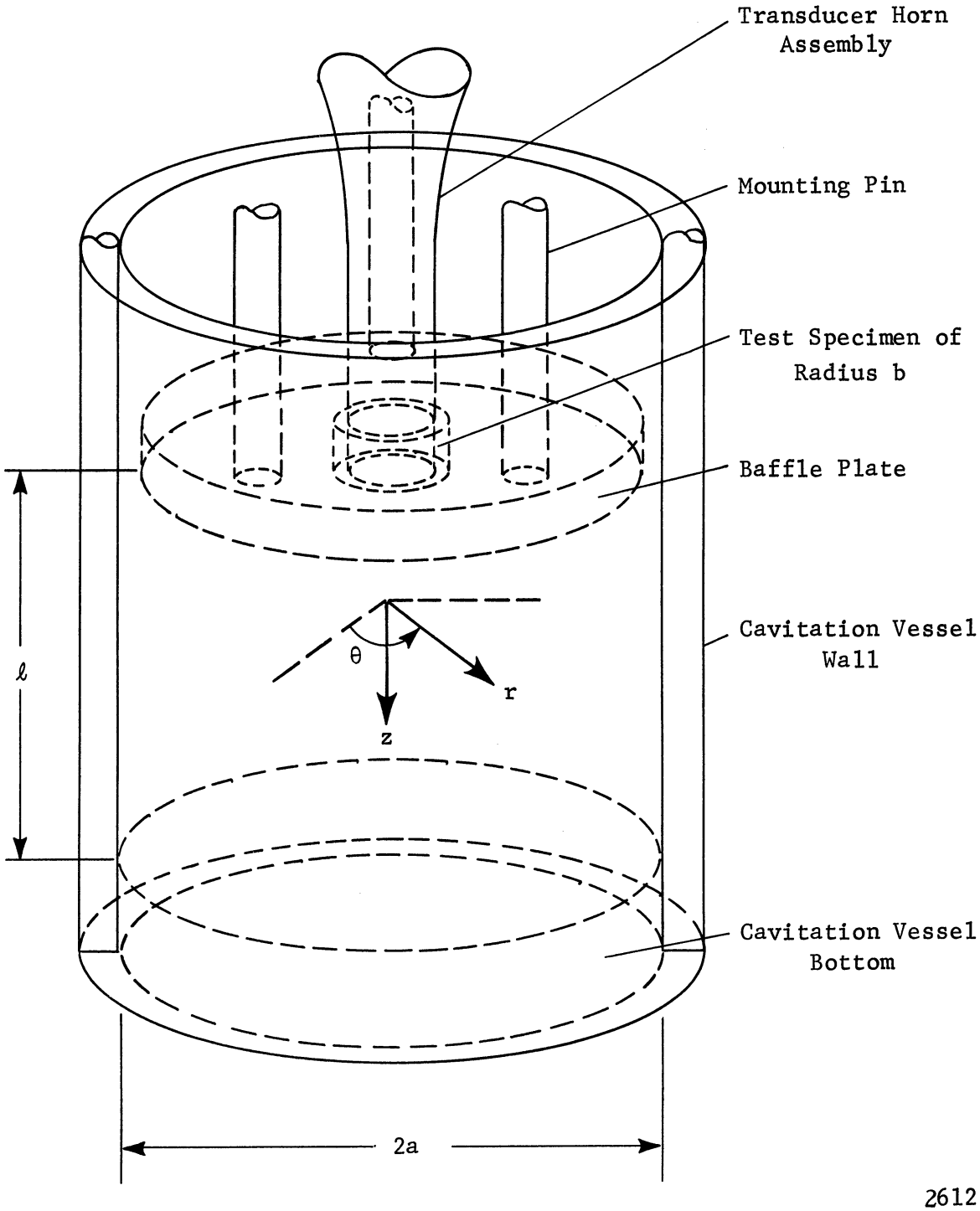

Figure 3. Cavitation Vessel, Baffle Plate, and Transducer Horn Assembly

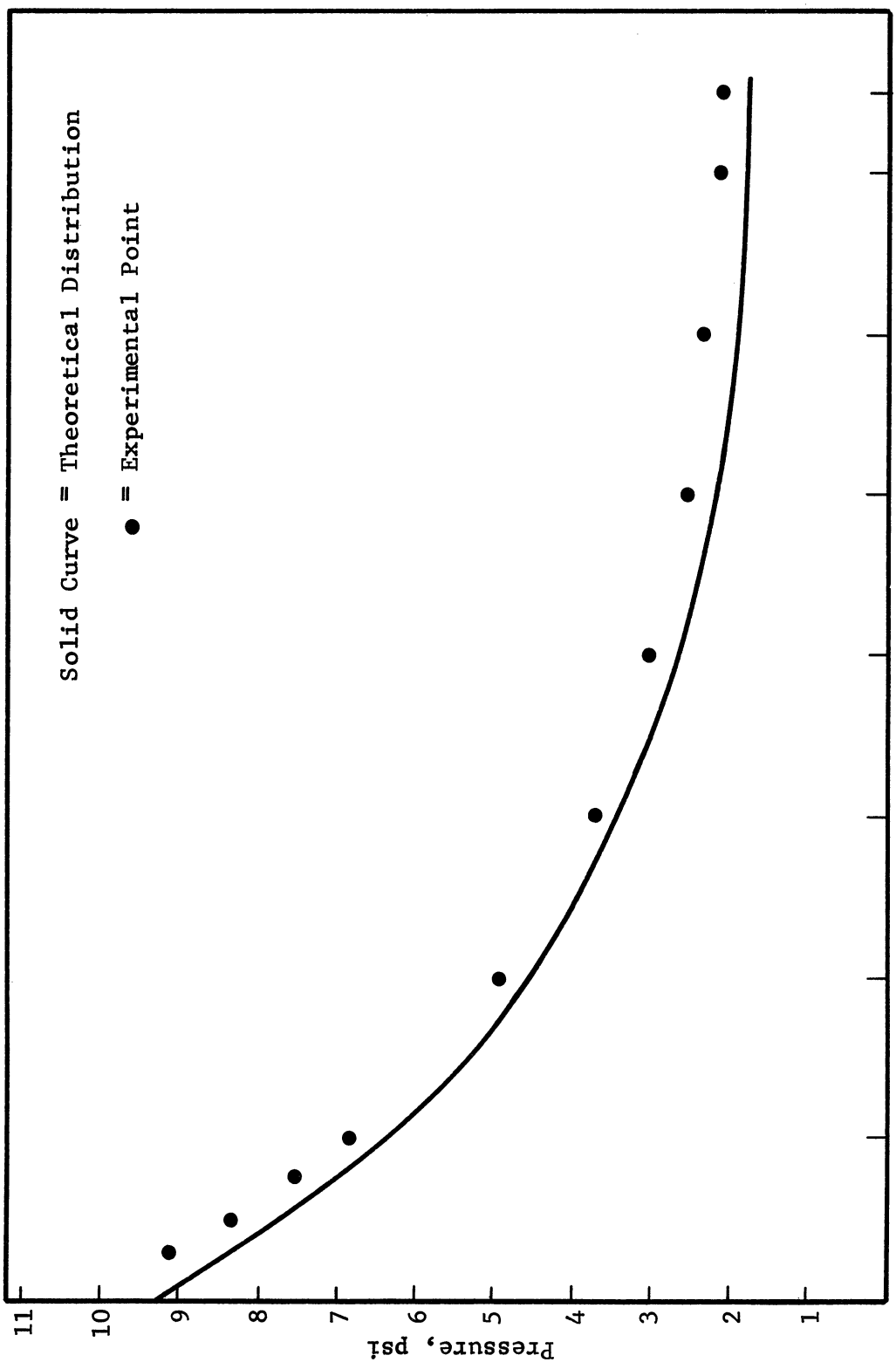

Figure 4. Pressure Distribution in Z Direction for r = 0, ℓ = .75 inches, Frequency = 14498 Hz, and A = 4.43×10^{-5} inches

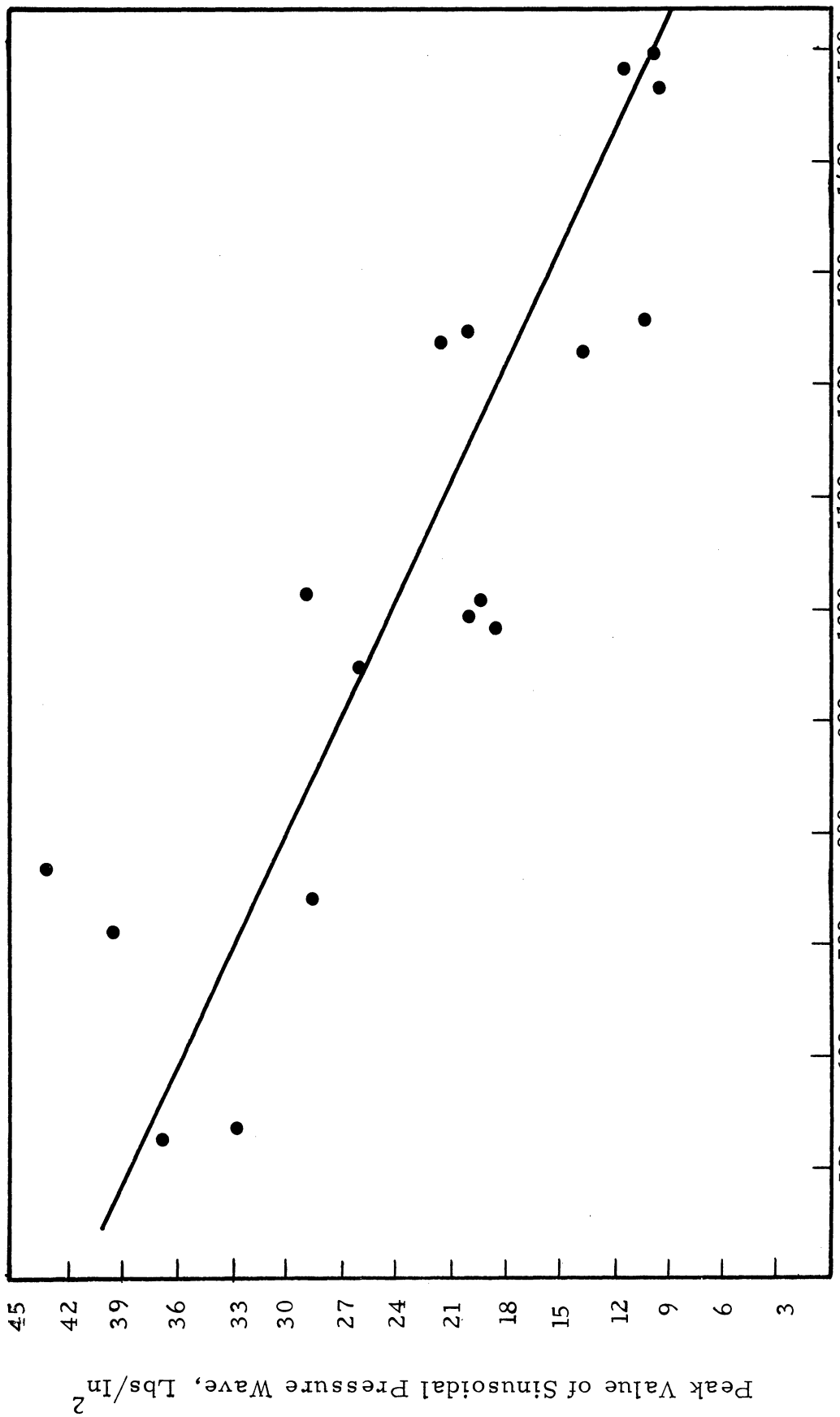

Figure 5. Peak Value of Sinusoidal Pressure Wave in Liquid Sodium Using 14 kHz Transducer Horn Assembly

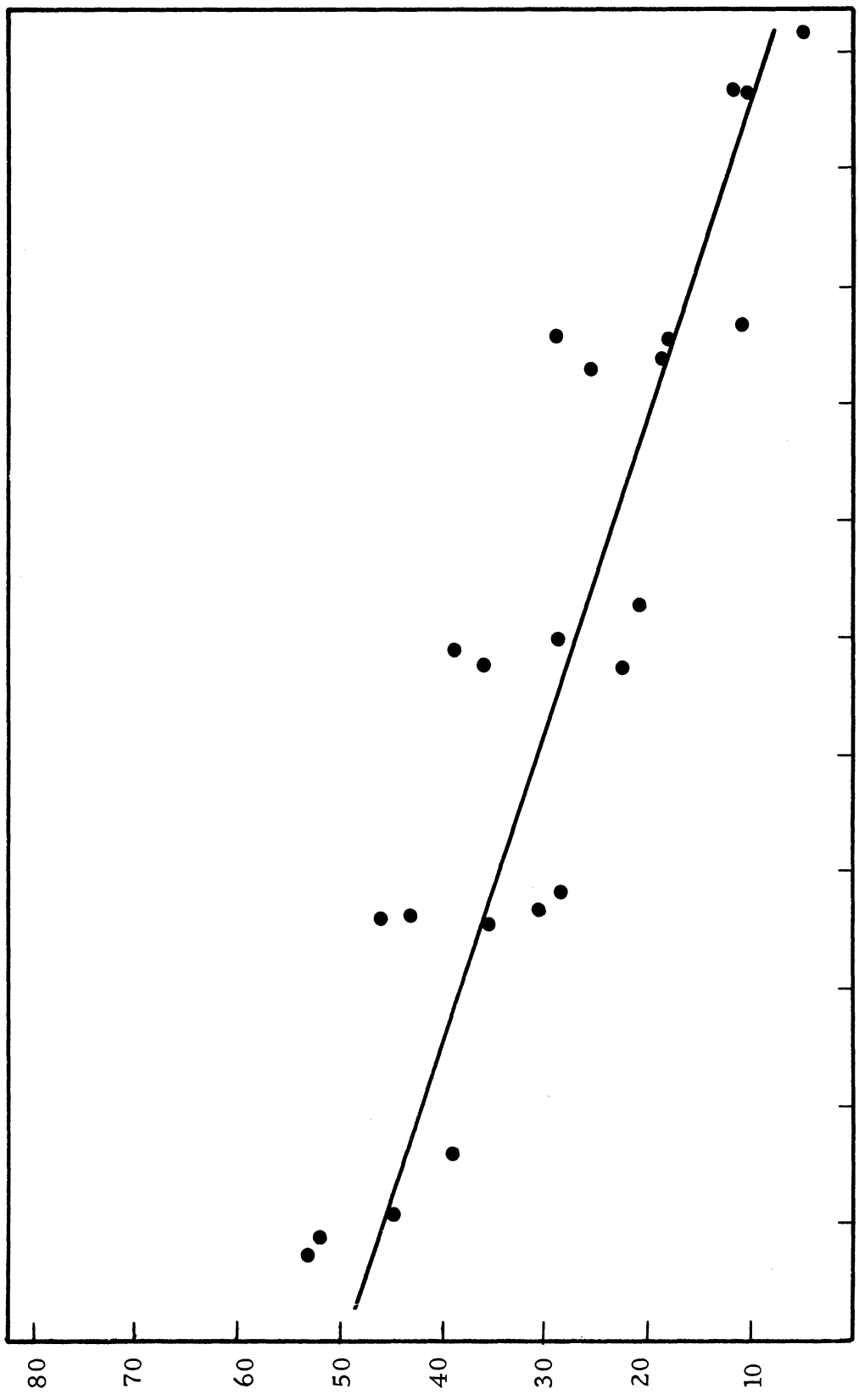

Figure 6. Peak Value of Sinusoidal Pressure Wave in Liquid Sodium Using 20 kHz Transducer Horn Assembly

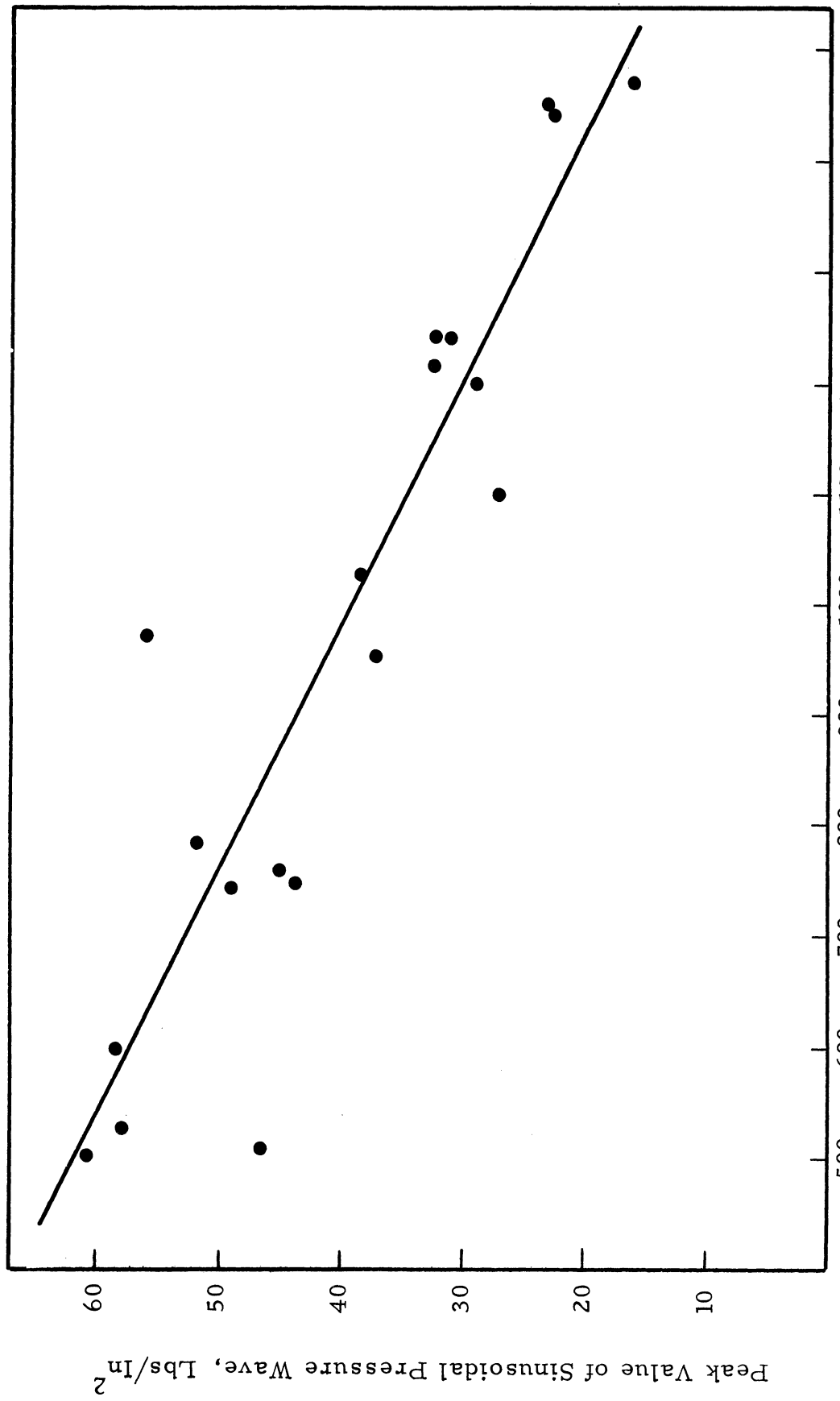

Figure 7. Peak Value of Sinusoidal Pressure Wave at Onset of Cavitation in Liquid Sodium Using 22 kHz Transducer Horn Assembly

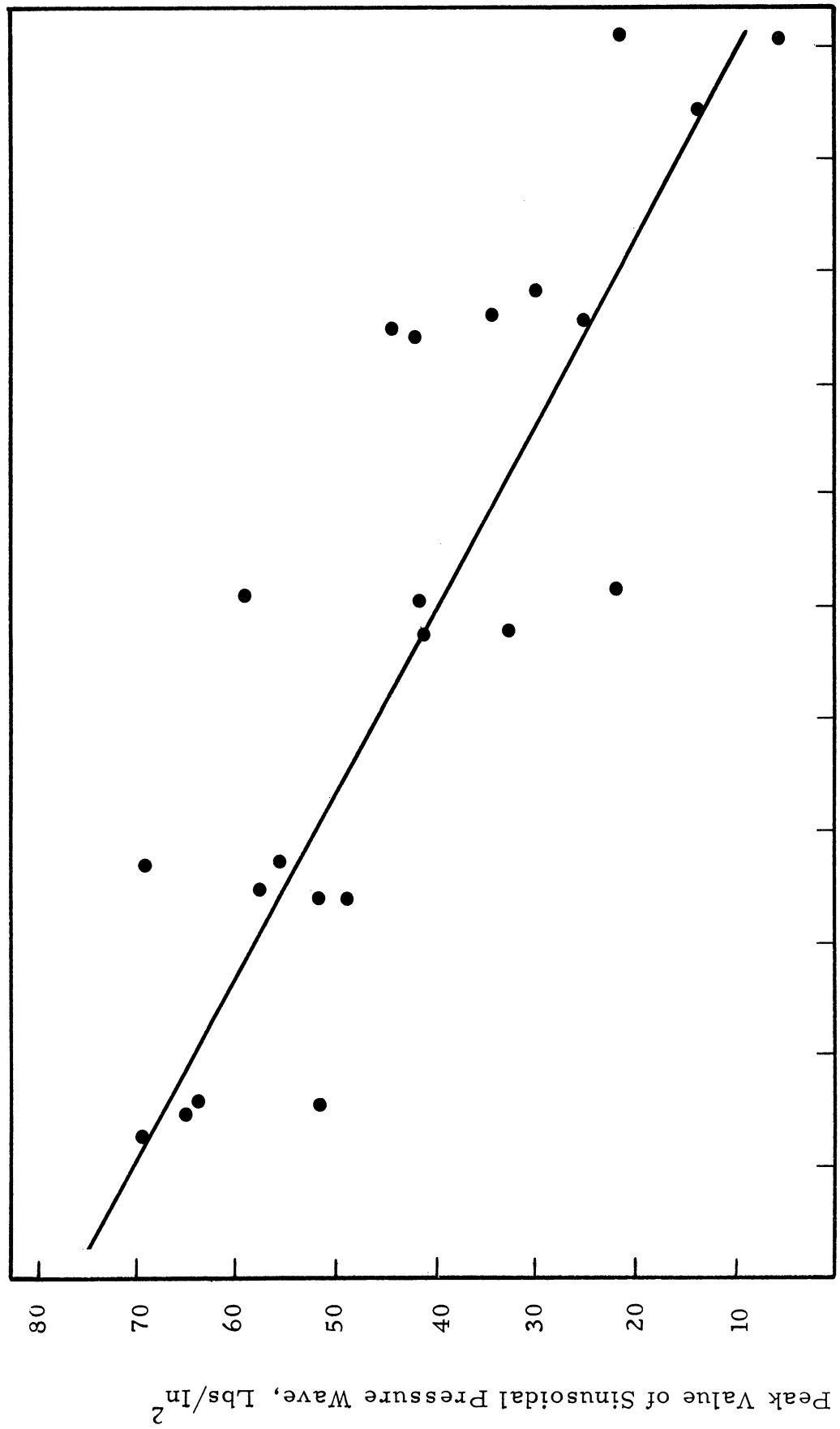

Figure 8. Peak Value of Sinusoidal Pressure Wave at Onset of Cavitation in Liquid Sodium Using 25 kHz Transducer Horn Assembly

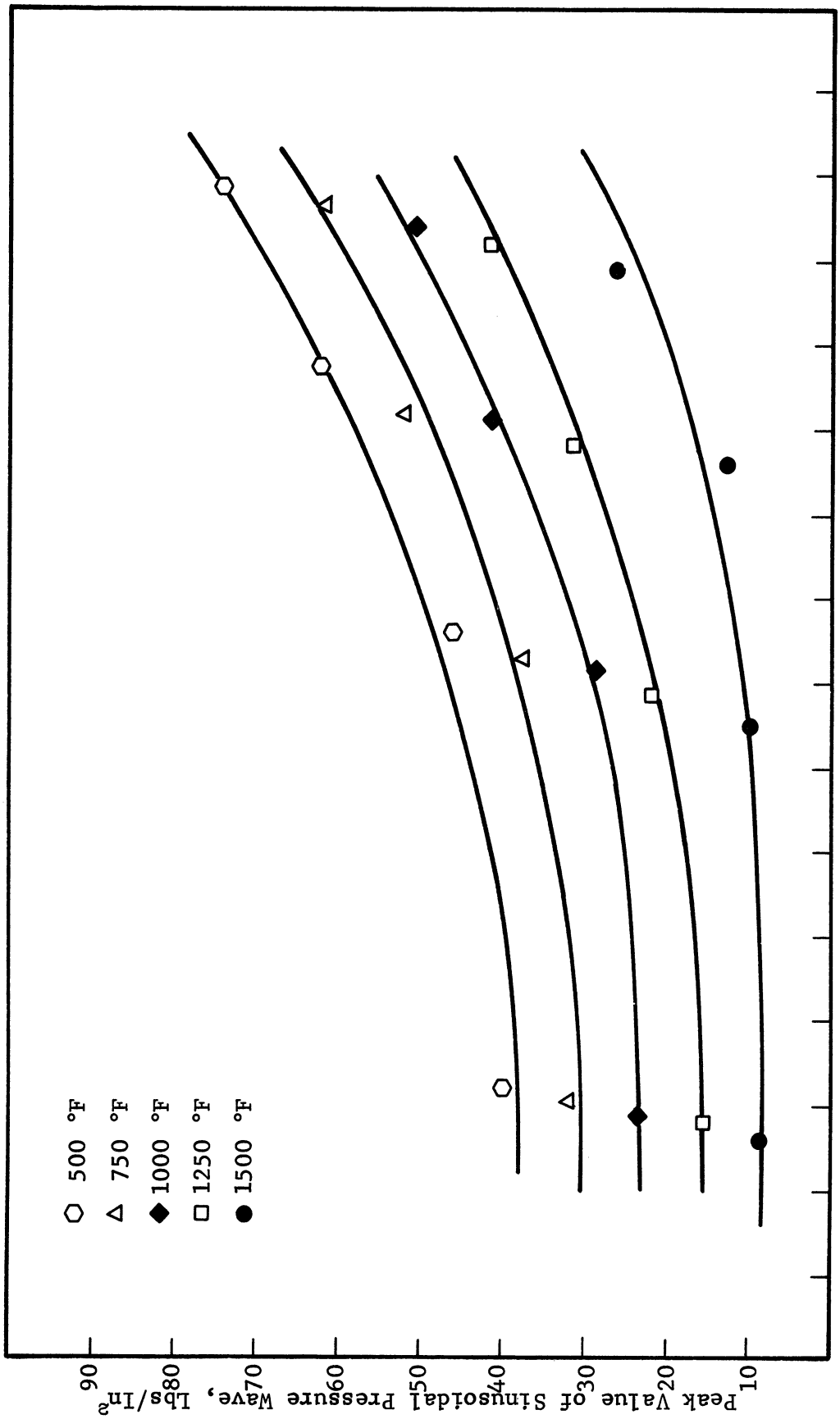

Figure 9. Peak Value of Sinusoidal Pressure Wave at Onset of Cavitation Versus Frequency for Liquid Sodium Temperatures 500, 750, 1000, 1250, and 1500°F

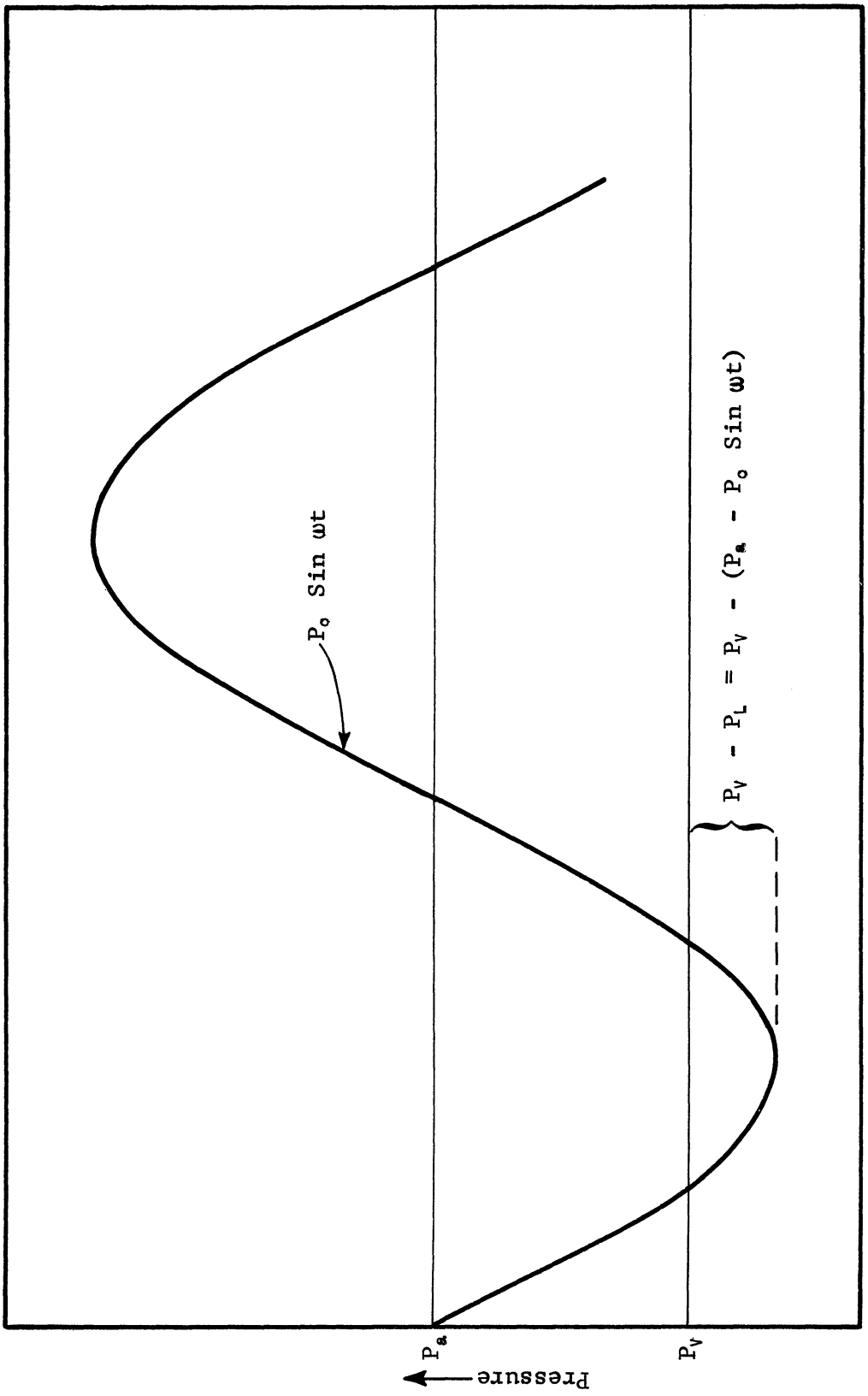

2656

Figure10. Relationships Among Atmospheric Pressure, P_a, Vapor Pressure, P_v, and Applied Sinusoidal Pressure Field, P_o sin ωt

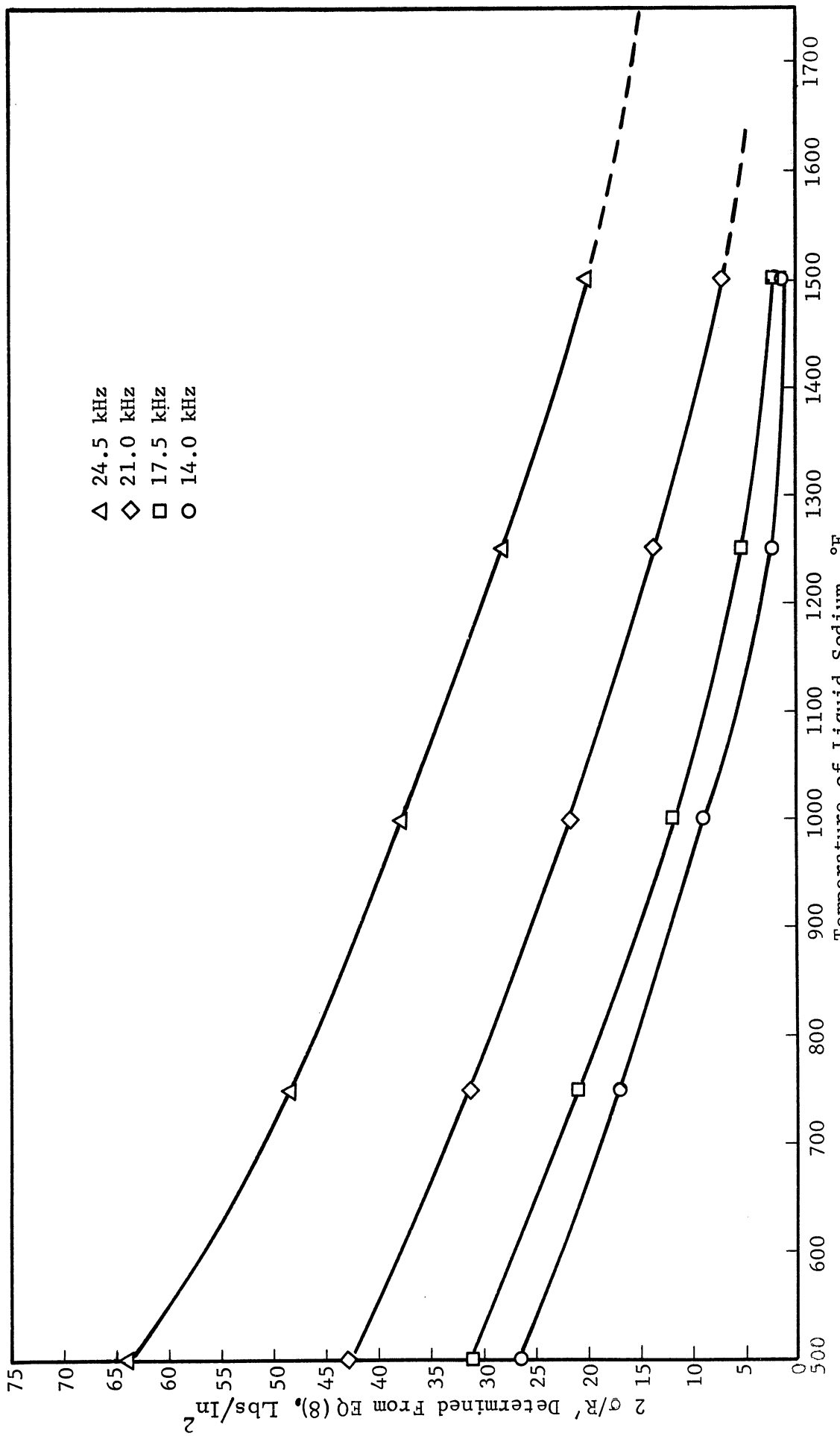

Figure 11. $2\sigma/R'$ Versus Temperature of Liquid Sodium at the Onset of Cavitation for 14, 17.5, 21, and 24.5 kHz

2.657

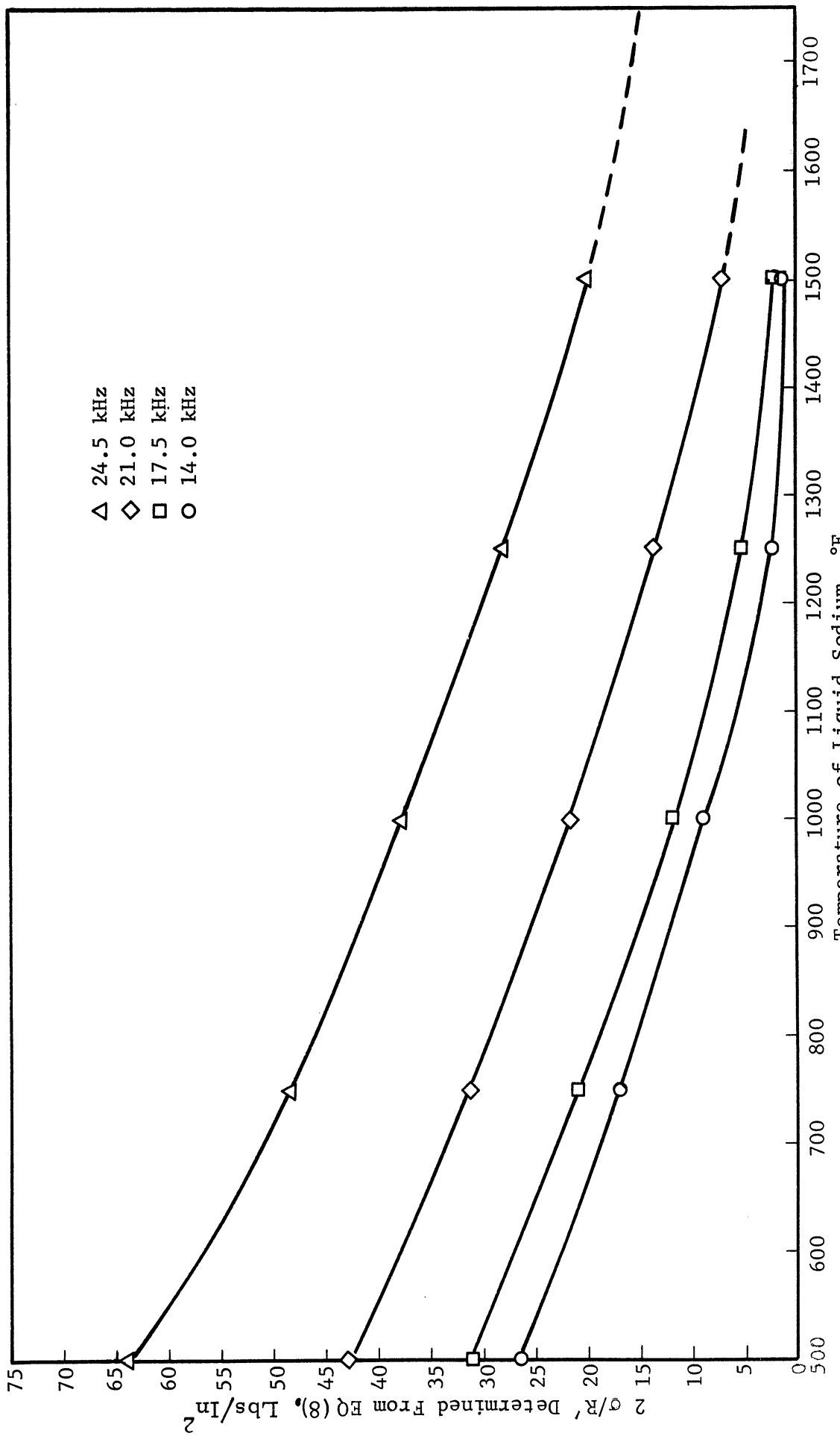

Figure 11. $2\sigma/R'$ Versus Temperature of Liquid Sodium at the Onset of Cavitation for 14, 17.5, 21, and 24.5 kHz

2.657

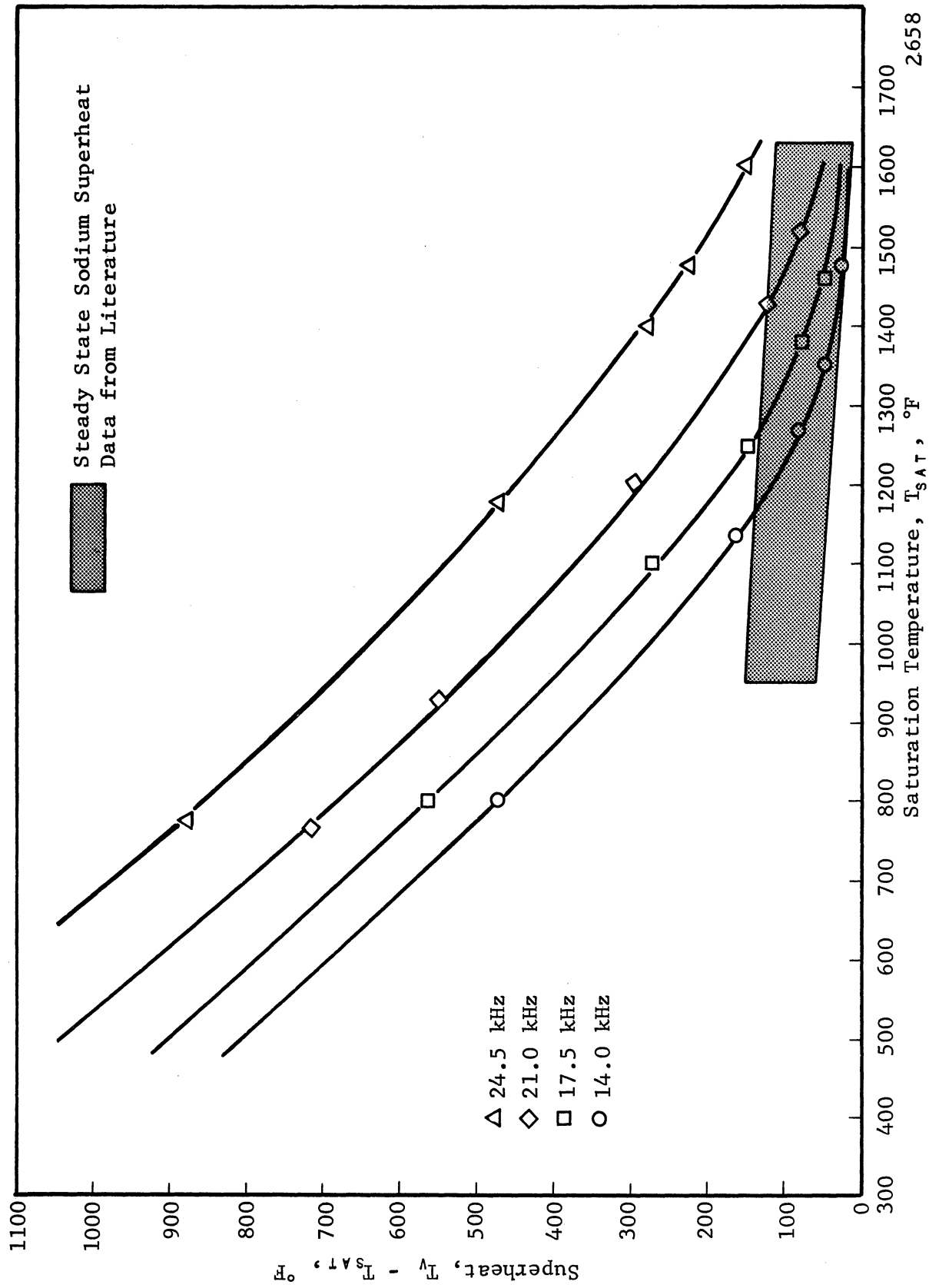

Figure 12. Liquid Sodium Superheat Versus Saturation Temperature for 14.0, 17.5, 21.0, and 24.5 kHz

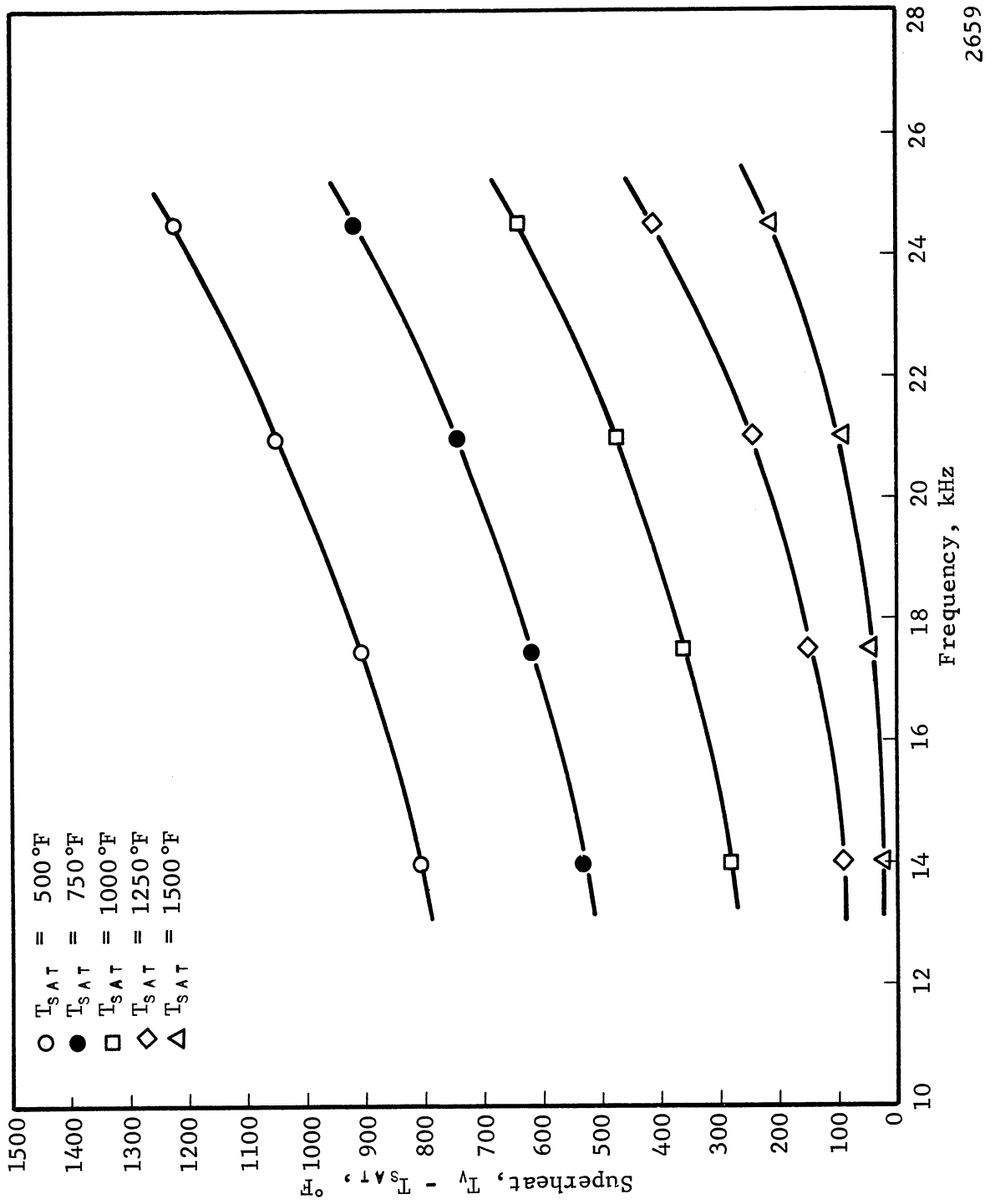

Figure 13. Liquid Sodium Superheat Versus Frequency for Saturation Temperatures 500, 750, 1000, 1250, and 1500°F

TABLE 1

Analysis of Sodium Used in This Experiment and Analysis of Sodium Used in the Enrico Fermi Nuclear Reactor

Impurity	Concentration Found In Sodium Used In Experiment	Concentration Found In Sodium Used in Fermi Reactor
Oxygen	22-25 ppm	5-25 ppm
Total Hydrogen Content	3.6 ppm	1-5 ppm
Total Carbon Content	33-50 ppm	20-200 ppm

TABLE 2

Numerical Values Used in the Calculation of Sodium Superheat

Freq. kHz	T_v °F	P_v^* psi	$2\sigma/R'_o$ ** psi	R'_o cm x 10^4	P_L psi	T_{sat} * °F	$T_v - T_{sat}$ °F
14.0	1500	7.88	1.10	31.7	6.78	1473	27
14.0	1400	4.28	1.15	31.5	3.13	1353	47
14.0	1350	3.06	1.30	29.7	1.76	1271	79
14.0	1300	2.12	1.55	24.5	0.57	1120	180
14.0	1275	1.80	1.78	21.7	0.02	821	454
17.5	1500	7.88	1.70	20.7	6.18	1458	42
17.5	1450	5.85	2.15	16.7	3.70	1376	74
17.5	1400	4.27	2.75	13.2	1.52	1252	148
17.5	1370	3.54	3.10	11.9	0.44	1105	265
17.5	1361	3.32	3.30	11.3	0.02	821	540
21.0	1600	13.28	4.70	7.03	8.58	1515	85
21.0	1550	10.18	5.60	6.05	4.58	1410	140
21.0	1500	7.88	6.80	5.17	1.08	1207	293
21.0	1485	7.27	7.20	4.94	0.07	925	560
21.0	1484	7.22	7.21	4.93	0.01	775	709
24.5	1750	27.82	14.10	2.22	13.72	1608	142
24.5	1700	22.00	15.20	2.09	6.80	1476	224
24.5	1675	19.56	15.70	2.05	3.86	1383	292
24.5	1650	17.12	16.30	2.00	0.82	1173	477
24.5	1642	16.51	16.50	1.99	0.01	775	867

* Obtained from reference (12)

** Obtained from Fig. 11